

## LUMINESCENCE PROPERTIES OF ZINC NIOBIUM TELLURIUM GLASSES DOPED THULIUM OXIDE

Y. M. ABOU DEIF<sup>a</sup>, M. M. ALQAHTANI<sup>a</sup>, A. M. EMARA<sup>a</sup>, H. ALGARNI<sup>a,b</sup>,  
E. S. YOUSEF<sup>a, b\*</sup>

<sup>a</sup>Department of Physics, Faculty of Sciences, King Khalid University, P. O. Box 9004, Abha, Saudi Arabia

<sup>b</sup>Research Center for Advanced Materials Science (RCAMS), King Khalid, University, Abha 61413, P. O. Box 9004, Saudi Arabia.

In this paper, the tellurite glasses  $76.4\text{TeO}_2\text{-}12\text{Nb}_2\text{O}_5\text{-}12.6\text{ZnO}$  doped with 3000ppm  $\text{Tm}_2\text{O}_3$  ions were prepared by conventional melt quenching method. The optical properties of the glasses were estimated by measuring UV-Vis-NIR spectroscopy in the range from 200 to 2500 nm and linear refractive indices ( $n$ ) at different wavelength was estimated. From the absorption edge studies, the value of optical band gap ( $E_{opt}$ ) was determined. Moreover, the nonlinear refractive index ( $n_2$ ), third-order nonlinear susceptibility ( $\chi^{(3)}$ ), and nonlinear absorption coefficient, ( $\beta$ ), were observed. It is noticed that ( $n_2$ ),  $\chi^{(3)}$  and  $\beta$  increase by decreasing the value of optical band gap ( $E_{opt}$ ). The classical McCumber theory was used to evaluate the emission cross-sections for the  ${}^3\text{F}_4 \rightarrow {}^3\text{H}_6$  transition at a wavelength of around  $2\mu\text{m}$ . Gain cross-section for the  $\text{Tm}^{3+}$  laser transition  ${}^3\text{F}_4 \rightarrow {}^3\text{H}_6$  was obtained. These glasses have the effective emission cross section bandwidth (108 nm) and large stimulated emission cross-section ( $28.37 \times 10^{-21} \text{cm}^2$ ). Spectroscopic properties indicate that these glasses doped with  $\text{Tm}^{3+}$  are a promising candidate for optical applications and may be suitable for optical fibre lasers and amplifiers. Furthermore, the structures of these glasses were analyzed by Raman spectroscopy.

(Received February 14, 2018; Accepted April 24, 2018)

**Keywords:**  $\text{TeO}_2$ ; Linear refractive indices, Emission cross section; Gain.

### 1. Introduction

Newly, much interest has been played to  $\text{Tm}^{3+}$  doped glasses due to their optical properties for several applications, such as optical reading, atmospheric sensing, some applications in medical surgery and eye-safe laser radar [1–4]. Most of the investigations on  $\text{Tm}^{3+}$  ions have been focused on their four metastable multiplets  ${}^3\text{F}_4$ ,  ${}^3\text{H}_4$ , which emit in the NIR region and  ${}^1\text{G}_4$ ,  ${}^1\text{D}_2$  which emit mainly in the visible region. Especially interesting is the emission at  $1.8\mu\text{m}$  which is attribute to the  ${}^3\text{F}_4 \rightarrow {}^3\text{H}_6$  transition and the blue emission ( ${}^1\text{D}_2 \rightarrow {}^3\text{F}_4$ ) which could be used for visible lasers. However, the host material is one of the important issues that need to be considered. Amongst the potential candidates as hosts, tellurite glasses of far several advantages including ease and low production cost in comparison to single crystal counter parts, high chemical stability and a wide transmission range from ultraviolet to mid-infrared ( $0.35\text{--}5.0\mu\text{m}$ ) [5–7]. In comparison to silicate and phosphate glasses, tellurite glasses have lower melting temperature [8,9], a higher refractive index [10], a good infrared transmittance [11] as well as smaller phonon energy that reduces the effect of non-radiative decay and therefore results in higher luminescence quantum efficiencies. Furthermore, the solubility of rare earth oxides is much higher than in  $\text{SiO}_2$  glasses [12].

This work presents a study of the optical properties of tellurite glasses doped with 3000ppm. The emission cross sections determined using the McCumber theory. Furthermore, the structure of these glasses was analyzed by Raman spectroscopy.

---

\* Corresponding author: [omn\\_yousef2000@yahoo.com](mailto:omn_yousef2000@yahoo.com)

## 2. Experimental Procedure

Tellurite glasses with the molar composition 76.4TeO<sub>2</sub>- 12Nb<sub>2</sub>O<sub>5</sub>-12.6ZnO in mol% (TNZ: Tm) was prepared by melt quenching technique from the raw materials TeO<sub>2</sub>- Nb<sub>2</sub>O<sub>5</sub>-ZnO and Tm<sub>2</sub>O<sub>3</sub>, which all were used as high purity reagents (> 99.99%). The powder was mixed and heated in a platinum crucible in the furnace at 950 °C for 45min. Subsequently, the highly viscous melt was cast to a graphite mould. The quenched glass was annealed at 300 °C for 2 hours, then slowly cooled down to room temperature. The glasses sample was cut and polished to different geometries for spectroscopic studies and optical measurements. The thickness of the studied samples is L =4.51 mm. The density of the glasses was measured using helium pycnometer (AccuPyc1330, Micromeritics GmbH, Germany) with an accuracy of ±0.0001 g/cm<sup>3</sup>.

The structure of this tellurite glass was studied using a Raman spectrometer (Senterra, Bruker GmbH, Germany) under an excitation of 514 nm. The transmission spectrum was measured using a Fourier transform spectrometer Vector 22 (Bruker GmbH, Germany). The absorption spectrum was recorded at wavelengths in the range of 190–2500nm using UV/Vis/NIR spectrophotometer 3101PC (Shimadzu, Japan) error of about 1%.

## 3. Results and discussion

### 3.1. Refractive index and density

Linear refractive indices measured at the wavelengths 436, 480, 546, 589 and 644nm are 3.3701, 3.0939, 2.8511, 2.7497 and 2.6579, respectively (shown in Fig.1). The refractive index is affected by many factors such as the electronic polarizability of the ions which are included in the glasses composition and the optical basicity of the glasses.

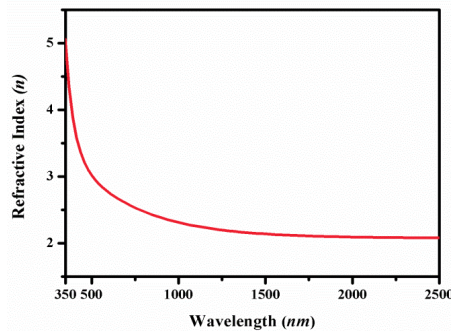


Fig. 1. Variation of refractive index as a function of wavelength for the TNZ doped with Tm<sup>3+</sup> ions.

On the other hand, the linear refractive index depends on the wavelength and it is given by the wimple equation [13].  $\frac{1}{n^2(E)-1} = \frac{E_s}{E_d} - \frac{E^2}{E_s E_d}$ , where E is the light energy (= hv), E<sub>s</sub> is called Sellmeier gap which is usually considered as the energy separation between the centers of both the conduction and the valence bands energy and E<sub>d</sub> is the dispersion energy or the average oscillator strength. This latest measures the average strength of interband transitions. From the linear regression of the curve 1/(n<sup>2</sup>-1) vs. E<sup>2</sup> (see Fig. 2), values for E<sub>d</sub> and E<sub>s</sub> of 18.34 and 3.88eV, are respectively obtained.

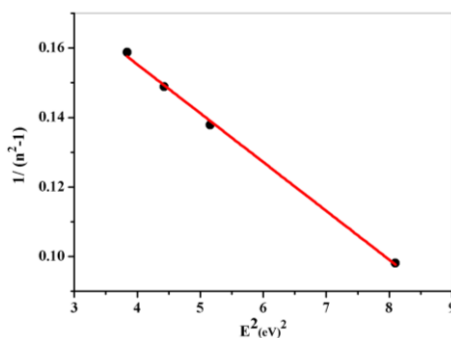


Fig.2: Dependency of the refractive index on the photon energy (illustrated as  $1/(n^2-1)$  vs.  $(E)^2$ ) of the TNZ glass doped with  $Tm^{3+}$  ions

The third order nonlinear susceptibility,  $\chi^{(3)}$ , of glasses according to the theory of Lines [14,15] and Kim et al. [16] can be calculated as follows:

$$\chi^3 = 25 \times 10^{-13} \cdot \frac{\left(\frac{f \cdot (n_0^2 + 2)}{3}\right)^3 \cdot d^2 \cdot (n^2 - 1) \cdot E_s^6}{n_0 [E_s^2 - E^2]^4},$$

where:  $f$  is the local field enhancement factor and  $d$

is the bond length between cation and anion, in angstrom. The nonlinear refractive indices  $n_2$  is related to  $\chi^3$  by the following relation:  $\chi^3 \text{ (esu)} = n_0/3\pi \cdot n_2 \text{ (esu)}$ . The  $|n_2|$  values and  $\chi^{(3)}$  of  $92.9 \times 10^{-15} \text{ (cm}^2/\text{w)}$  and  $143.6 \times 10^{-13} \text{ (esu)}$ , respectively. The two photon non-linear absorption coefficient (TPA),  $\beta$  can be calculated using the following expression:  $\beta = KE_p^{1/2} F/n^2 E_g^3$  [17- 20]; where  $F$  is the function which represents the dispersion of  $\beta$  with respect to the incident photon energy  $h\nu$ , with:  $F = [2h\nu - E_g/E_g]^3/2 / [2h\nu/E_g]$ , and  $K = 3100 \text{ cm GW}^{-1}$ ;  $E_p = 21 \text{ eV}$  is the Kane energy parameter. The photon energy  $h\nu$  range is selected at wavelength satisfying the two-photon absorption TPA condition:  $E_g/2 < h\nu < E_{opt}$ . If the glasses have high nonlinear absorption coefficient this leads to promising properties for nonlinear optical devices such as power limiters, real time holography, ultrafast optical switches, self focusing and white light continuum generation. In the present work, the value of  $\beta$  is  $4.38 \text{ cm GW}^{-1}$ . In the glasses with the compositions  $76\text{TeO}_2\text{-}20\text{Nb}_2\text{O}_5\text{-}4\text{BaO}$  and  $60\text{TeO}_2\text{-}10\text{Bi}_2\text{O}_3\text{-}30\text{WO}_3$ , the value of,  $\beta$ , was reported as 1.72 and 0.565, respectively. By using femto-second Z-scan method at 800 nm the value of  $\beta$  for  $\text{TeO}_2\text{-} \text{Bi}_2\text{O}_3\text{-} \text{BaO}$  and  $\text{TeO}_2\text{-} \text{Bi}_2\text{O}_3\text{-} \text{TiO}_2$  glasses were obtained; they were in range from 1.037 to 4.141  $\text{cm GW}^{-1}$  and from 0.599 to 1.483  $\text{cm GW}^{-1}$ , respectively [21, 22]. So the present glasses should have promising properties for the above mentioned applications.

The optical absorption edge is an important parameter for describing solid-state materials and it is interpreted in terms of direct or indirect transitions across an optical bandgap. The absorption coefficient,  $\alpha(\omega)$ , is given by [23]:  $\alpha(\omega) = \frac{A(\hbar\omega - E_{opt})^r}{\hbar\omega}$ , where  $\alpha(\omega)$  is the absorption coefficient,  $A$  is constant,  $E_{opt}$  is the optical band edge and  $\hbar\omega$  is the photon energy of the incident radiation. The exponent,  $r$ , is takes different value which depend on the mechanism of the interband transition [24]. The,  $E_{opt}$ , is estimated by extrapolating from the linear regions of the curves  $(\alpha\hbar\nu)^{1/2}$  vs.  $\hbar\nu$  as shown in Fig. 3. The value of optical energy gap equals to 2.7eV. This comparatively high value of the optical energy gap provides the possibility that these glasses may be suitable for optical device components.

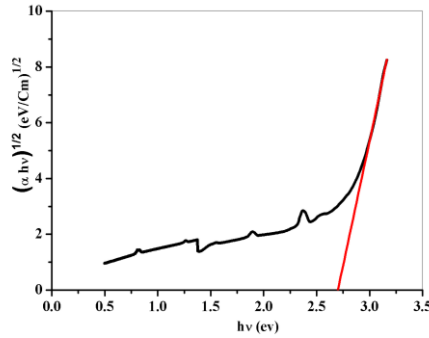


Fig. 3.  $(\alpha h\nu)^{1/2}$  as a function of  $h\nu$  for the TNZ doped with  $Tm^{3+}$  ions.

The density of TNZ:Tm glasses is determined to be  $\rho = 5.381 \pm 0.0026$  g/cm<sup>3</sup> that can be used to calculate the concentration of  $Tm^{3+}$  ions by the relation:  $N = [RE \text{ mol}\%] \frac{\rho}{M} 2A_V$ , Where [RE mol%] is the molar percentage of rare-earth oxide based on the molar mass of the glasses composition, M is the molecular weight of the TNZ:Tm glasses. The concentration of  $Tm^{3+}$  in the doped TNZ glass is  $N = 1.176581 \times 10^{20}$  ions/cm<sup>3</sup>.

### 3.2. Absorption spectroscopy, emission cross section and gain coefficient

The Judd–Ofelt (JO) theory is widely used for predicting the possibility of laser action, as well as of optical amplification, through an analysis of the forced electric dipole transitions within the  $4f^n$  configuration of rare-earth ions in different isotropic lattices (crystalline and amorphous) [25–27]. The absorption spectrum of 3000ppm $Tm_2O_3$  doped TNZ glasses, which is obtained at room temperature over a spectral range of 200–2500nm is shown in Fig. 4. The absorption spectrum is characterized by five bands centered at 1726, 1214, 794, 686 and 468 nm, corresponding to the absorptions starting from the ground state  $^3H_6$  to the excited states  $^3F_4$ ,  $^3H_5$ ,  $^3H_4$ ,  $^3F_3$  and  $^1G_4$ , respectively. The transitions to energy levels higher than  $^1G_4$  are not observed because of the intrinsic conduction band absorption of the host glass.

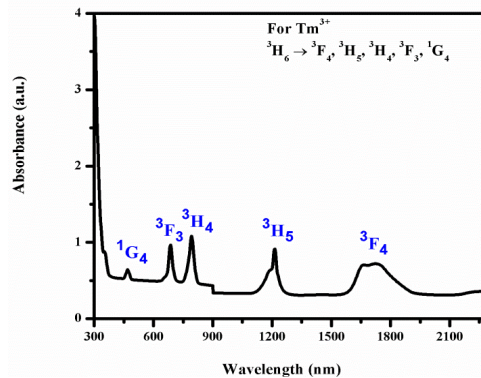


Fig. 4. UV–vis–NIR absorption spectrum of TNZ: Tm glass.

The absorption cross-sections of the  $Tm^{3+}$  ion for the  $^3F_4 \rightarrow ^3H_6$  transition can be calculated as follows:  $\sigma_a(\lambda) = \frac{2.303 \cdot OD(\lambda)}{NL}$ , Where  $OD(\lambda) = \log(I_0/I)$  is the optical density of the experimental absorption spectrum, L is the thickness of the sample and N is the concentration of respective rare-earth ions.

The stimulated emission cross-section  $\sigma_e(\lambda)$  of  $Tm^{3+}$  for the  $^3F_4 \rightarrow ^3H_6$  transition can be deduced from their corresponding ground state absorption cross-section  $\sigma_a(\lambda)$  using the following

equation [28]:  $\sigma_e(\lambda) = \sigma_a(\lambda) \frac{Z_l}{Z_u} \exp \left[ \frac{E_{Zl} - hc\lambda^{-1}}{K_B T} \right]$ , Where  $Z_l$  and  $Z_u$  are the partition functions for the lower and the upper levels involved in the considered optical transition, T is the temperature (in this case the room temperature), and  $E_{Zl}$  is the zero line energy for the transition between the lower Stark sublevels of the emitting multiplets and the lower Stark sublevels of the receiving multiplets.

Fig.5 shows the calculated absorption and emission cross sections for the present glasses. The peak of the stimulated emission cross-section ( $\sigma_e^{Peak}$ ) is about  $28.37 \times 10^{-21} \text{ cm}^2$  respectively. The highest value of ( $\sigma_e^{Peak}$ ) for the emission cross-section is related to the larger value of the line strength of the  ${}^3F_4 \rightarrow {}^3H_6$  and may be due to the higher refractive index of the glasses matrix.

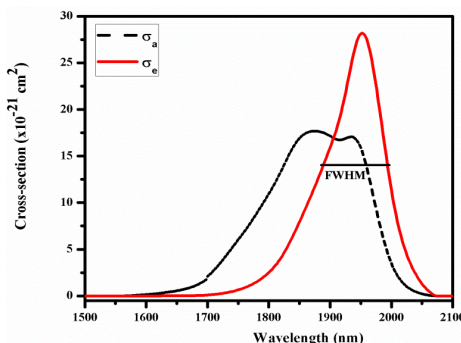


Fig. 5. absorption cross-sections  $\sigma_a(\lambda)$  and stimulated emission cross-sections  $\sigma_e(\lambda)$  of the transition  ${}^3H_6 \leftrightarrow {}^3F_4$  in TNZ: Tm.

The comparison value of the emission cross of the  $\text{Tm}^{3+}$  transition  ${}^3H_6 \leftrightarrow {}^3F_4$  in various glass hosts at around  $2\mu\text{m}$  of the TNZ:Tm glasses ( $28.37 \times 10^{-21} \text{ cm}^2$ ) is larger than those of other glasses (TNZ: Sm [29], Gallate [30], Germanate [31], Bismuthate [32], PZC: Er [33] and PZS: Er [33]) ( $1.09 \times 10^{-20}$ ,  $3.8 \times 10^{-21}$ ,  $7.7 \times 10^{-21}$ ,  $6.7 \times 10^{-21}$ ,  $0.47 \times 10^{-20}$  and  $0.39 \times 10^{-20} \text{ cm}^2$ ). For laser glasses, it is generally desirable for the emission cross section to be as large as possible in order to provide high gain [34]. It indicates that the doped glasses TNZ:Tm is a promising candidate for laser glass at  $2\mu\text{m}$  and  $1952 \text{ nm}$ . The FWHM of the emission peak is also a critical parameter that is used to evaluate the gain bandwidth properties of the optical amplifiers is  $110 \text{ nm}$  respectively.

Due to the large overlap of the absorption and emission spectrum of  $\text{Tm}^{3+}$  ions at  $2 \mu\text{m}$ , re-absorption will occur and cause the fluorescence spectrum deformed. Thus, due to the asymmetric profile of the emission line, it is more reasonable to calculate an effective line width, instead of the FWHM. The effective line width ( $\Delta\lambda$ ) can be expressed as  $\Delta\lambda = \int \sigma_e(\lambda) d\lambda / \sigma_e^{Peak}$ . The effective bandwidth is  $108 \text{ nm}$  respectively. The ground state presents a larger Stark splitting than the emitting level for the tellurite glass under study, in a similar way as in previous reports on  $\text{Er}^{3+}$  doped tellurite glasses [35]. The results also indicate that the bandwidth is strongly dependent on the overall extent of the Stark splitting.

The optical gain coefficient is an important factor for evaluating the performance of laser media. The light field intensity derived from the light field power by the simplified relationship  $I(Z) = \frac{P(Z)}{A}$ , where  $P(Z)$  is pump power at the position Z and A is an effective cross sectional area of the core. The propagation equation for the pump and signal field power  $P(Z)$  in a given direction are thus [36,34]:  $\frac{dP(Z)}{dz} = [\sigma_e N_2(Z) - [\sigma_a N_1(Z)] P(Z)]$ , Where N is total population volume-density and defined as  $N = N_1 + N_2$ ,  $N_1$  and  $N_2$  represent the population volume-densities of upper and lower levels, respectively. From the absorption and emission cross sections for the transitions between two laser operating levels, the optical gain cross section  $\sigma_{\text{gain}}$  that lead to an estimation of the probable operating laser wavelength. If P is the population inversion rate for  ${}^3F_4 \rightarrow {}^3H_6$ ,  $\text{Tm}^{3+}$  laser transition, the gain cross section can be calculated using the following relation:  $\sigma_{\text{gain}} = P \sigma_{\text{em}}(\lambda) - (1 - P) \sigma_{\text{abs}}(\lambda)$ , where  $\sigma_{\text{em}}$  and  $\sigma_{\text{abs}}$  are emission and absorption cross section,

respectively. The wavelength dependence of the gain cross section was calculated for different values of population inversion  $P$  ( $P = 0, 0.1, 0.2, \dots, 1$ ) and are shown in fig.6.

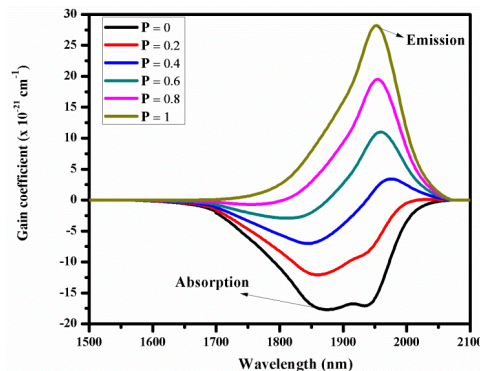


Fig. 6. The gain coefficient of the transition  ${}^3F_4 \rightarrow {}^3H_6$  for TNZ: Tm glass.

In the case of total inversion at 1952nm, again coefficient of  $28.5\text{cm}^{-1}$  is obtained for TNZ doped with 3000ppm  $\text{Te}_2\text{O}_3$  ions. But, as it is known for such laser systems, the inversion coefficient fraction is more likely close to 0.4 which leads to the gain coefficient values of  $3.5 \times 10^{-21}\text{cm}^{-1}$  at 1970nm. Laser experiments for these emissions are expected to find light amplification in the future.

### 3.3. Raman Spectra

Fig. 7 shows the spectrum of TNZ: Tm is deconvoluted using Gaussian fitting to four peaks at about  $409, 516, 686$  and  $800\text{cm}^{-1}$  which are labeled as A, B, C and D bands respectively. It show that abroad Raman band(A) at  $409\text{cm}^{-1}$  that are assigned to the symmetrical stretching or bending vibrations of Te–O–Te linkages which are formed by corner-sharing of  $(\text{TeO}_4)$ ,  $(\text{TeO}_{3+1})$  polyhedral and  $\text{TeO}_3$  units [37–39]. The peak (B) is ascribed to the axial symmetrical stretching modes of  $(\text{Te}_{\text{ax}}\text{--O})_s$  of  $\text{TeO}_4$  tetrahedra [40–43]. The band (C) is assigned to the  $(\text{Te}_{\text{eq}}\text{--O})_s$  and  $(\text{Te}_{\text{eq}}\text{--O})_{\text{as}}$  vibration modes of  $\text{TeO}_{3+1}$  polyhedra or  $\text{TeO}_3$  trigonal bipyramids units [44, 45] and peak (D) attributed to the stretching vibrations of Nb – O bonds in  $\text{NbO}_6$  octahedra [45].

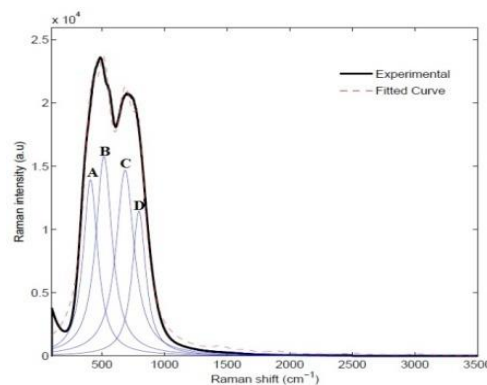


Fig. 7. Deconvoluted Raman spectra of TNZ: Tm glass.

## 4. Conclusion

The optical properties of the glasses were estimated by measuring UV–Vis–NIR spectroscopy. Indirect optical band gap energy value is 2.7eV. The present glasses have the high absorption intensities, emission cross-sections. The optical gain coefficient of the population inversion of the  ${}^3F_4$  level ( $3.5 \times 10^{-21}\text{cm}^{-1}$ ) and an effective bandwidth of 108nm for glasses has

been evaluated. The spectroscopic data obtained that the TNZ:Tm glasses can be used as a candidate for optical devices around at 2 $\mu$ m.

### Acknowledgements

This work was support of King Khalid University, the Ministry of Education, Kingdom of Saudi Arabia for this research through a grant (RCAMS-KKU-001-17) under research center for advanced material science.

### References

- [1] Ming Li, Gongxun Bai, Yanyan Guo, Lili Hu, Junjie Zhang, J. Lumin. **132**, 1830 (2012).
- [2] S. D. Jackson, S. Mossman, Appl. Phys. B: Lasers Opt **77**(5), 489 (2003).
- [3] Y. Tsang, A. El-Taher, T. King, K. Chang, S. Jackson, Opt. Lett. **31**, 6190 (2006).
- [4] D. F. de Sousa, L. F. C. Zonetti, M. J. V. Bell, J. A. Sampaio, L. A. O. Nunes, M. Baesso, A. C. Bento, L. C. M. Miranda, Appl. Phys. Lett. **74**(4), 908 (1999).
- [5] J. S. Wang, E. Snitzer, E. M. Vogel, J. G. H. Sigel, J. Lumin. **60-61**, 145 (1994).
- [6] J. S. Wang, E. M. Vogel, E. Snitzer, Opt. Mater. **3**, 187 (1994).
- [7] Dandan Yin, Yawei Qi, Shengxi Peng, Shichao Zheng, Fen Chen, Gaobo Yang, Xunsi Wang, Yaxun Zhou, J. Lumin. **146**, 141 (2014).
- [8] Rongrong Xu, Ying Tian, Lili Hu, Junjie Zhang, J. Non-Cryst. Solids **357**, 2489 (2011).
- [9] S. Shen, A. Jha, X. Liu, M. Naftaly, K. Bindra, H. J. Bookey, A. K. Kar, J. Am. Ceram. Soc. **6**, 1391 (2002).
- [10] K. Damak, R. Maâlej, E. Yousef, A. Qusti, C. Rüssel, J. Non-Cryst. Solids **358**, 2974 (2012).
- [11] Heike Ebdorff-Heidepriem, Kevin Kuan, Michael R. Oermann, Kenton Knight, Tanya M. Monro, Opt. Mater. Express **2**, 432 (2012).
- [12] R. A. H. El-Mallawany, CRC Press, Boca Ratan, FL (2002).
- [13] S. H. Wemple, J. Chem. Phys. **67**, 2151 (1977).
- [14] M. E. Lines, Phys. Rev. B **41**, 3383 (1990).
- [15] M. E. Lines, Phys. Rev. **69**, 6876 (1991).
- [16] S. H. Kim, T. Yoko, J. Am. Ceram. Soc. **78**, 1061 (1995).
- [17] M. Sheik-Bahae, D. J. Hagan, E. W. Van Stryland, Phys. Rev. Lett. **65**, 96 (1990).
- [18] M. Sheik-Bahae, E. W. Van Stryland, Semiconductors and semimetals, in: E. Garmire, A. Kost (Eds.), Academic, San Diego **58**, Chap. 4 (1999).
- [19] M. Weiler, Solid State Commun. **39**, 937 (1981).
- [20] B.S. Wherrett, J. Opt. Soc. Am. B **1**, 67 (1984).
- [21] Tiefeng Xu, Feifei Chen, Shixun Dai, Xiang Shen, Xunsi Wang, Qihua Nie, Chao Liu, Kai Xu, Jong Heo, J. Non-Cryst. Solids **357**, 2219 (2011).
- [22] Feifei Chen, Tiefeng Xu, Shixun Dai, Qihua Nie, Xiang Shen, Jianliang Zhang, Xunsi Wang, Opt. Mater **32**, 868 (2010).
- [23] E. Yousef, M. Hotzel, C. Rüssel, J. Non-Cryst. Solids **353**, 333 (2007).
- [24] Kamel Damak, El Sayed Yousef, Christian Rüssel, Ramzi Maâlej, J. Quant. Spectrosc. Radiat. Transf. **134**, 55 (2014).
- [25] H. Lin, S. Tanabe, L. Lin, Y.Y. Hou, K. Liu, D.L. Yang, T.C. Ma, J.Y. Yu, E.Y.B. Pun, J. Lumin. **124**, 167 (2007).
- [26] B. R. Judd, Phys. Rev. **127**, 750 (1962).
- [27] G. S. Ofelt, J. Chem. Phys. **37**, 511 (1962).
- [28] X. Zou, H. Toratani, Phys. Rev. B, **52**, 511 (1995).
- [29] A. M. Emara, M. M. Alqahtani, Y. M. AbouDeif, El Sayed Yousef, J. Chalco., Letters, **14**(9), 405 (2017).
- [30] B. Peng, T. Izumitani, Opt. Mater. **4**, 797 (1995).
- [31] R. Balda, L. M. Lacha, J. Fernandez, J. M. Fernandez-Navarro, Opt. Mater.

27,1771 (2005).

[32] H. Fan, G. Gao, G. Wang, J. Hu, L. Hu, *Opt. Mater.* **32**,627 (2010).

[33] B. Afef, Moteb M. Alqahtani, H.H. Hegazy, E. Yousef, K. Damak, R. Maâlej, *J. of Luminescence*,**194**,706 (2018).

[34] Ju H. Choi, Frank G. Shi, Alfred. Margaryan, Ashot. Margaryan, Wytze van der Veer, *J. Alloys Comp.* **450**,540 (2008).

[35] D. E. McCumber, *Phys. Rev.* **136**,954 (1964).

[36] Xujie. Li, Wenjie. Zhang, *Phys. B.* 403 (2008) 3286.

[37] G. Upender, V.G.Sathe, V.C.Mouli, *Phys.Chem.Glasses***50**, 399 (2009).

[38] C. Duverger, M.Bouazaoui, S.Turell, *J.Non-Cryst.Solids***220**, 169 (1997).

[39] S. Suresh, M.Prasad, GUpender, V.Kamalaker, V.CMouli, *IndianJ.PureAppl. Phys.***47**, 163 (2009).

[40] V. Ravikumar, N. Veeraiyah, *J.Phys.Chem.Solids***59**, 91 (1998).

[41] G. Amarnath, S.Buddhudu, F.G.Brayant, *J.Non-Cryst.Solids***122**, 66 (1990).

[42] T.Sekiya, N.Mochida, A.Soejima, *J.Non-Cryst.Solids***191**, 115 (1995).

[43] B.V.R Choudari, P.PramodaKumari, *Mater.Res.Bull.***34**, 327 (1999).

[44] K. Fukimi, S.Sakka, *J.Mater.Sci.***23**, 2819 (1988).

[45] G. Upender, S.Ramesh, M.Prasad, V.G.Sathe, V.ChandraMouli, *J.Alloy. Compd.* **504**468 (2010).